(4)

AFGL-TR-87-0245
ENVIRONMENTAL RESEARCH PAPERS, NO. 963

Ionospheric Scintillations/TEC and In-Situ Density Measurements at an Auroral Location in the European Sector

EILEEN MACKENZIE
SANTIMAY BASU
SUNANDA BASU

14 August 1987

IONOSPHERIC PHYSICS DIVISION PROJECT 4643
AIR FORCE GEOPHYSICS LABORATORY
HANSCOM AFB, MA 01731

"This technical report has been reviewed and is approved for publication."

SANTIMAY BASU
Author

WILLIAM K. VICKERY
Acting Branch Chief

FOR THE COMMANDER

WILLIAM K. VICKERY
Acting Division Director

This document has been reviewed by the ESD Public Affairs Office (PA) and is releasable to the National Technical Information Service (NTIS).

Qualified requestors may obtain additional copies from the Defense Technical Information Center. All others should apply to the National Technical Information Service.

If your address has changed, or if you wish to be removed from the mailing list, or if the addressee is no longer employed by your organization, please notify AFGL/DAA, Hanscom AFB, MA 01731. This will assist us in maintaining a current mailing list.

Do not return copies of this report unless contractual obligations or notices on a specific document requires that it be returned.

Unclassified

SECURITY CLASSIFICATION OF THIS PAGE

REPORT DOCUMENTATION PAGE

Form Approved OMB No. 0704-0188

1a. REPORT SECURITY CLASSIFICATION: Unclassified	1b. RESTRICTIVE MARKINGS: None
2a. SECURITY CLASSIFICATION AUTHORITY	3. DISTRIBUTION/AVAILABILITY OF REPORT: Approved for public release; distribution unlimited.
2b. DECLASSIFICATION/DOWNGRADING SCHEDULE	
4. PERFORMING ORGANIZATION REPORT NUMBER(S): AFGL-TR-87-0245 ERP, No. 983	5. MONITORING ORGANIZATION REPORT NUMBER(S)
6a. NAME OF PERFORMING ORGANIZATION: Air Force Geophysics Laboratory 6b. OFFICE SYMBOL (If applicable): LIS	7a. NAME OF MONITORING ORGANIZATION
6c. ADDRESS (City, State, and ZIP Code): Hanscom AFB Massachusetts 01731-5000	7b. ADDRESS (City, State, and ZIP Code)
8a. NAME OF FUNDING/SPONSORING ORGANIZATION 8b. OFFICE SYMBOL (If applicable)	9. PROCUREMENT INSTRUMENT IDENTIFICATION NUMBER
8c. ADDRESS (City, State, and ZIP Code)	10. SOURCE OF FUNDING NUMBERS PROGRAM ELEMENT NO.: 61102F; PROJECT NO.: 4643; TASK NO: 09; WORK UNIT ACCESSION NO.: 03

11. TITLE (Include Security Classification)
Ionospheric Scintillations/TEC and In-Situ Density Measurements at an Auroral Location in the European Sector

12. PERSONAL AUTHOR(S)
Eileen MacKenzie*, Santimay Basu, and Sunanda Basu*

13a. TYPE OF REPORT	13b. TIME COVERED	14. DATE OF REPORT (Year, Month, Day)	15. PAGE COUNT
Scientific Report	FROM 10/2/86 TO 7/31/87	1987 August 14	44

16. SUPPLEMENTARY NOTATION
This research was supported in part by Emmanuel College, Contract F19628-86-K-0038, and the Defense Nuclear Agency. *Emmanuel College, Boston, MA 02115

17. COSATI CODES		
FIELD	GROUP	SUB-GROUP

18. SUBJECT TERMS (Continue on reverse if necessary and identify by block number)
Amplitude and phase scintillations; Auroral oval; Total electron content; Sunspot cycle variation; In-situ density (Contd)

19. ABSTRACT (Continue on reverse if necessary and identify by block number)

The orbiting HiLat satellite launched by the Defense Nuclear Agency in 1983 offered a unique opportunity for studying the ionospheric scintillation parameters in relation to the in-situ measurements of ionization density, drift velocity, field-aligned current, and particle precipitation during the sunspot minimum period. This report discusses the results of a morphological study performed at the Air Force Geophysics Laboratory based on their observations of scintillations and total electron contents (TEC) at the auroral oval station at Tromso, Norway, during the period December 1983 - October 1985. A separate report will provide a morphology of in-situ medium scale (~ tens of km) density structures and ion velocity fluctuations at 830 km.

The geometrical enhancement of scintillations observed during the alignment of the propagation path with the local magnetic L-shell is shown to be the most consistent and conspicuous feature of scintillations in the nighttime auroral oval. The dynamics of the spatial and temporal extent of this region are illustrated in the invariant (Contd)

20. DISTRIBUTION/AVAILABILITY OF ABSTRACT	21. ABSTRACT SECURITY CLASSIFICATION
☐ UNCLASSIFIED/UNLIMITED ☒ SAME AS RPT. ☐ DTIC USERS	Unclassified
22a. NAME OF RESPONSIBLE INDIVIDUAL: Santimay Basu	22b. TELEPHONE (Include Area Code): (617) 377-3141; 22c. OFFICE SYMBOL: AFGL/LIS

DD Form 1473, JUN 86 — Previous editions are obsolete. SECURITY CLASSIFICATION OF THIS PAGE

Unclassified

18. (Contd)

Irregularity anisotropy
Decorrelation time
Phase spectral index

---

19. (Contd)

latitude/magnetic local time grid.

The steepening of phase spectral slope in the geometrical enhancement region is indicative of the presence of L-shell aligned sheet-like irregularities at long scale lengths. The seasonal variation of ~~total electron content~~ (TEC) determined from the differential Doppler measurements of HiLat transmissions is discussed in relation to the in-situ density measurements at 830 km. The results are also ~~utilized~~ to illustrate the dependence of ionospheric structure parameters on short-term variability of solar activity during the sunspot minimum period. This joint study of scintillation/TEC and in-situ parameters provides an insight into the nature of magnetospheric coupling with the ionosphere at high latitudes.

Preface

The authors would like to thank F. J. Rich of AFGL, the Principal Investigator of the plasma monitor on HiLat, for making his data available to us. We appreciate the efforts of R.C. Livingston of SRI International for his help with the radio beacon data analysis, Paul Pruneau of Boston College for the compilation of the large data base and statistics generation, and Nelson Bonito of AFGL for assistance with the color polar plot programming. The work was funded in part by the Defense Nuclear Agency. The work at Emmanuel College was supported by AFGL Project 4643 under Contract F19628-86-K-0038.

Contents

Illustrations

Illustrations

Tables

Ionospheric Scintillations/TEC and In-Situ Density Measurements at an Auroral Location in the European Sector

1. INTRODUCTION

A wide variety of C^3I systems suffer degradation in performance due to phase and intensity scintillations imposed by the ionospheric irregularities of electron density. Earlier publications (Aarons)[1] have documented the morphological features of major scintillation regions. Long-term studies have predominantly utilized intensity scintillation measurements (Basu and Basu;[2] Basu and Aarons;[3] Aarons et al[4]). The DNA Wideband satellite made possible phase scintillation observations at the equator (Livingston)[5] and the auroral oval in both the Alaskan sector

(Received for publication 12 August 1987)

1. Aarons, J. (1982) Global morphology of ionospheric scintillations, Proc. IEEE, 70:360.
2. Basu, S., and Basu, Su. (1981) Equatorial scintillations - A review, J. Atmos. Terr. Phys., 43:473.
3. Basu, Su., and Aarons, J. (1980) The morphology of high-latitude VHF scintillations near 70° W, Radio Sci., 15:59.
4. Aarons, J., Mullen, J.P., Whitney, H., Johnson, A., and Weber, E. (1981) VHF scintillation activity over polar latitudes, Geophys. Res. Lett., 8:277.
5. Livingston, R.C. (1980) Comparison of multifrequency equatorial scintillation: American and Pacific sectors, Radio Sci., 15:801.

(Rino and Matthews)[6] and the North Atlantic sector (Basu et al)[7]. Since the Wideband satellite was sun-synchronous, observations were available only near local midnight and in the pre-noon hours. To extend the diurnal coverage, phase scintillation measurements utilizing Fleetsat (Basu et al[8]) and a quasi-stationary polar beacon satellite (Basu et al[9]) have been presented.

There is a great deal of interest in understanding the development of such irregularities at high latitudes where the ionosphere is often strongly coupled with the magnetosphere. In such an environment the distant magnetosphere serves to activate different sources of free energy, for example, electron precipitation, field-aligned currents, electric fields, and so on, that control the formation of ionospheric irregularities. No longer is it possible to pursue a study of the irregularity development in the local ionospheric environment without considering the coupling between the ionosphere and the magnetosphere. This approach is particularly useful in extrapolating our knowledge of the natural ionospheric irregularity structures to problems related to the structuring of artificially injected plasma clouds in the high latitude ionosphere.

In an effort to study plasma structuring in the above context, the Defense Nuclear Agency (DNA) launched, on 27 June 1983, the HiLat satellite in a circular 830-km orbit at 82° inclination. The satellite transmits coherent signals at 137, 390, 413, and 436 MHz and the phase reference signal at 1239 MHz to measure complex signal scintillation and total electron content (TEC). It also carries a variety of in-situ probes providing measurements of ion density, ion drift, energetic electron precipitation, field-aligned currents, and emissions at two visible wavelengths. All instruments except the Langmuir probe, the vacuum-ultraviolet imager and a part of the magnetometer continue to operate reliably. Table 1 [reproduced from Fremouw and Wittwer[10]] lists the instruments and the experimenters.

---

6. Rino, C.L., and Matthews, S.J. (1980) On the morphology of auroral zone radio wave scintillation, J. Geophys. Res., 85:4139.

7. Basu, Su., Basu, S., Livingston, R.C., Whitney, H.E., and MacKenzie, E. (1981) Comparison of Ionospheric Scintillation Statistics From the North Atlantic and Alaskan Sectors of the Auroral Oval Using the Wideband Satellite, Rep. AFGL-TR-81-0266, ADA 111871, Air Force Geophysics Laboratory, Hanscom AFB, MA.

8. Basu, Su., Basu, S., Livingston, R.C., MacKenzie, E., and Whitney, H.E. (1982) Phase and Amplitude Scintillation Statistics at 244 MHz From Goose Bay Using a Geostationary Satellite, Rep. AFGL-TR-82-0222, ADA 124291, Air Force Geophysics Laboratory, Hanscom AFB, MA.

9. Basu, Su., Basu, S., MacKenzie, E., and Whitney, H.E. (1985) Morphology of phase and intensity scintillations in the auroral oval and polar cap, Radio Sci., 20:347.

10. Fremouw, E.J., and Wittwer, L.A. (1984) The HiLat satellite program: introduction and objections, Johns Hopkins APL Technical Digest, 5:98.

Table 1. HiLat Experiments
(Reproduced from Fremouw and Wittwer[10])

Instrument	Observations	Operating Characteristics	Experimenters
Coherent beacon	Scintillation Total electron content	Phase-coherent radio-wave signals at 138, 390, 413, 436 and 1239 MHz; circular polarization.	Carlson (Air Force Geophysics Laboratory) Forsyth (University of Western Ontario) [3]Fremouw (Physical Dynamics, Inc.) [4]Rino (SRI International)
Plasma monitor	Ion and electron concentration Dominant ion species Ion and electron temperature Electric field	[1]Langmuir probe: electron concentration and temperature; spectral density of concentration irregularities at 3, 10, 35, 500, and 750 m wavelengths. Retarding potential analyzer: ion concentration and in-track ion velocity, 3.5 km resolution; temperature and mass of dominant ion. Ion drift meter: cross-track drift velocity field with 880 m resolution.	[4]Rich (Air Force Geophysics Laboratory) Heelis, Hanson (University of Texas, Dallas)
Vector magnetometer	Magnetic field Electric current along magnetic field lines	Three-axis fluxgate: 13 nT quantizations, 400 m resolution.	[4]Potemra (APL)
Electron spectrometer	Electron flux and energy spectra	Energy range: 20 eV to 20 keV; three look directions: up, down, and 45° from zenith. Three modes, spatial resolution 300, 600, and 1800 m.	[4]Hardy (Air Force Geophysics Laboratory)
Auroral Ionospheric Mapper	Night and day auroral and F-layer emissions	[2]1150 to 2000 Å imaging spectrophotometer. Wavelength resolution: 30 Å; spatial resolution in E (F) layer is 5 × 20 km (3 × 13 mi) at nadir. 3914 and 6300 Å nadir-viewing photometers.	[4]Huffman (Air Force Geophysics Laboratory) Meng (APL)

[1]Not fully operable.

[2]Imager failed on 23 July 1983.

[3]HILAT Project Scientist.

[4]Experiment principal investigator.

L. A. Wittwer (Defense Nuclear Agency), Program Manager

The major objective of the HiLat satellite program is to provide a quantitative specification of high latitude scintillation strength and, in particular, the temporal and spatial spectra of intensity and phase fluctuations and the shape of the irregularity structures. These parameters provided by the radio beacon experiments are supported by the simultaneous in-situ data that define the background ionospheric processes.

In this report we shall concentrate on the HiLat satellite observations performed by the Air Force Geophysics Laboratory at Tromso, Norway during the 1984-1985 period. The station is located in the central part of the auroral oval during the nighttime hours under magnetically quiet conditions as defined by the planetary magnetic index $Kp < 3.5$. We shall study the strength and the structure specifications of complex signal scintillations in the spatial and temporal frames of invariant latitude and magnetic local time. These distributions will then be examined in the context of in-situ plasma structures observed by the HiLat satellite in this environment and the theoretical predictions of structures that characteristically develop in this region through gradient drift and Kelvin-Helmholtz instability processes.

2. DATA

We shall illustrate the space-time variations of the statistical parameters that define the complex scintillation magnitudes and their structure over the two-year period December 1983 - October 1985. Scintillation measurements have been made on a sliding 30-sec window with values computed every 15 sec at the midpoint of the window over the length of each pass (approximately 10 min) and have been merged into seasonal data bases. To avoid the effects of multipath propagation, the data acquired above a satellite elevation angle of 20° were used in the study. This provided a maximum latitude coverage of about ± 7° at an ionospheric height of 350 km around the station. Due to the precession of the Hilat orbit to earlier times each day, a full coverage in local time is also obtained over a season (that is, three months) when the ascending and descending node passes are combined. The parameters discussed in this report are the 137-MHz phase and intensity scintillation observations and their associated spectral parameters, the total electron content, and the in-situ ion density measured at the height of the satellite. These statistical parameters used to quantify scintillations are analogous to those defined in earlier Wideband (Basu et al)[7] and Fleetsat (Basu et al)[8] reports. A short definition of each follows.

2.1 RMS Phase Deviation

The standard deviation of the linear detrended phase component over a 30-sec data interval is calculated as

$$\sigma_\phi = (\langle\phi^2\rangle - \langle\phi\rangle^2)^{1/2}$$

and is the phase scintillation parameter.

2.2 Phase Spectral Slope and Strength

The phase power spectral density ($\Phi_\phi(f)$) assumes a power law form as

$$\Phi_\phi(f) = T_\phi f^{-p_\phi}$$

where f is the fluctuation frequency, p_ϕ is the spectral slope and T_ϕ is the spectral strength in mks units. The slope is computed from a linear least-squares fit to the plot of the logarithm of $\Phi_\phi(f)$ vs the logarithm of frequency over the range 0.2 to 10 Hz. The spectrum is generated by a FFT algorithm with a cosine window on the 30-sec data sample.

2.3 Intensity Scintillation Index, S_4

The S_4 index was first introduced by Briggs and Parkin[11] and is the normalized second central moment of signal intensity:

$$S_4 = [(\langle I^2\rangle - \langle I\rangle^2)/\langle I\rangle^2]^{1/2}.$$

It ranges from 0 to ~1 for quiet to strong scatter conditions.

2.4 Decorrelation Time

Decorrelation time is computed as the time delay in seconds for the intensity signal to reach a decorrelation level of 0.5.

---

11. Briggs, B.H., and Parkin, I.A. (1963) On the variation of radio star and satellite scintillation with zenith angle, J. Atmos. Terr. Phys., 25:339.

The phase and intensity scintillation parameters pertain to the 350-km sub-ionospheric intersection point of the satellite as observed from Tromso. The total electron content (TEC) is measured up to 830 km, the height of the satellite, and the ion density is that measured at the height of the satellite, 830 km. A $(\sec i)^{1/2}$ correction for ionospheric zenith angle (i) was incorporated into the σ_ϕ and S_4 parameters while a (sec i) correction was used for TEC. Median values of the above mentioned parameters have been obtained in 2.5° invariant latitude - 1 hr MLT bins and will be presented in polar plot form in the following sections. A maximum of 150 data points are available in some invariant latitude-MLT bins but the majority of the bins have 50 data points. Bins with fewer than 10 data samples have been omitted to provide some statistical validity to the results.

The invariant latitude of the overhead position of Tromso is 66° Λ which corresponds to the central part of the nightside auroral oval. Figure 1 shows the station location at midnight with respect to the Q = 3 auroral oval (Feldstein and Starkov),[12] which is reproduced from Whalen.[13] This allows comparison of the day- and nightside auroral oval locations under quiet magnetic conditions with the band of latitudes for which data is available (usually 60° - 72.5° Λ). The invariant latitudes agree almost exactly with the corrected geomagnetic latitude (used for Figure 1) in this longitude sector (J.A. Whalen, private communication, 1984). Thus we note that the HiLat data from Tromso generally covers the nightside oval while the dayside oval is immediately poleward of the coverage from the station.

The seasonal data bases have been sorted into two groups: those observations made under magnetically quiet conditions (Kp < 3.5) and those under magnetically disturbed conditions (Kp > 3.5). The data sub-set under magnetically disturbed conditions (Kp > 3.5) is very limited. This constrains us to select only one season as the "worst case" and illustrate the median values for all the parameters during this season under conditions of Kp > 3.5.

---

12. Feldstein, Y.I., and Starkov, G.V. (1967) Dynamics of auroral belt and polar geomagnetic disturbances, Planet. Space Sci., 15:209.

13. Whalen, J.A. (1970) Auroral Oval Plotter and Nomograph for Determining Corrected Geomagnetic Local Time, Latitude and Longitude for High Latitudes in Northern Hemisphere, AFCRL-70-0422, AD 713170, Air Force Geophysics Laboratory, Hanscom AFB, MA.

AURORAL OVAL
(Feldstein and Starkov, 1967)

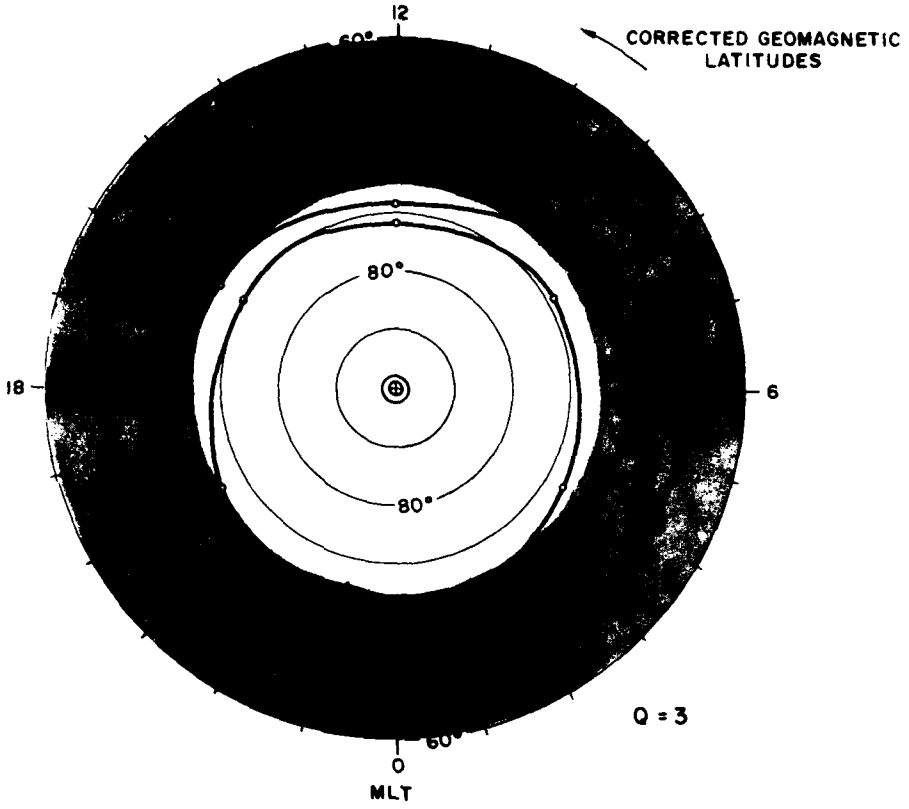

Figure 1. Polar Plot of Invariant Latitude and Magnetic Local Time Illustrating the Latitude Interval of Available Data With Respect to the Q= 3 Auroral Oval

One remaining, but very important, factor to be considered is the solar flux variation over the two-year period. Figure 2 illustrates the drastic variation of sunspot number for Dec 1983 - Oct 1985. As a reference, at the peak of the last sunspot cycle in the fall of 1979, sunspot numbers approached values of about 180 while in the fall of 1985, sunspot numbers decreased to values as low as 20.

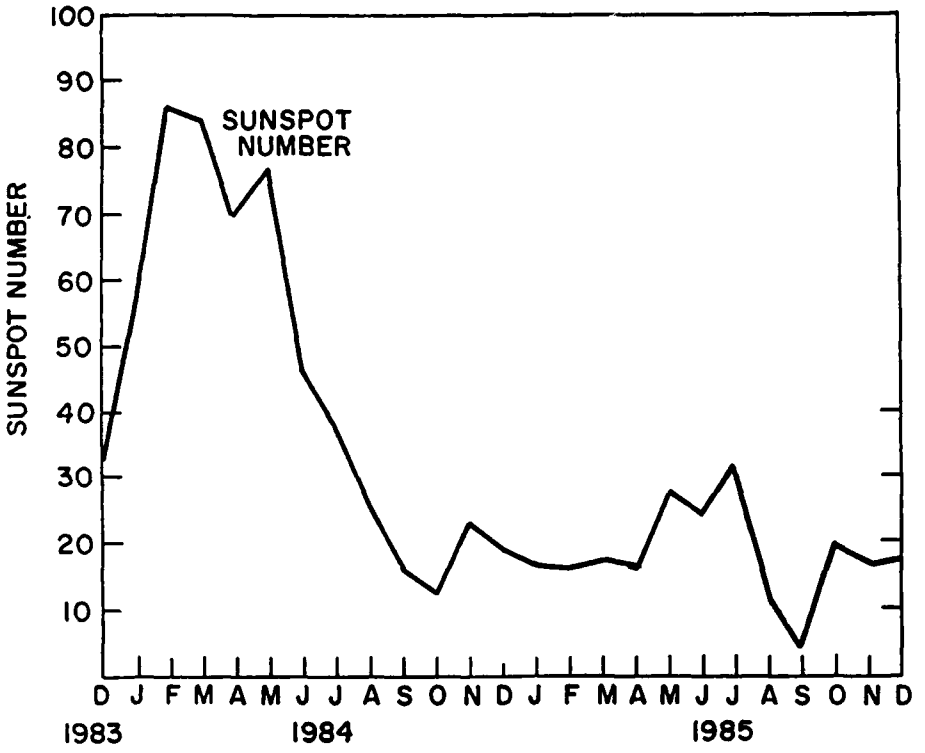

Figure 2. Variation of Monthly Mean Sunspot Number Between December 1983 and December 1985

3. RESULTS

3.1 RMS Phase Deviation

Figure 3 illustrates the rms phase deviation, σ_ϕ, of 137 MHz scintillation for winter 1983 (start of observations in Dec 1983 to Jan 1984), spring 1984 (Feb-Apr 1984), summer 1984 (May-Jul 1984) and fall 1984 (Aug-Oct 1984) for Kp < 3.5. The rms phase deviation is computed over a 30-sec data interval and the variation of the parameter with ionospheric zenith angle has been removed prior to statistical processing. Since the projected scan velocity of the satellite is approximately 3 km/sec at 350 km, the data interval covers irregularity scale sizes as large as 90 km. The data are binned in 2.5° latitude and 1 hr MLT intervals and the median values are indicated for each bin. Each bin contains at least ten data points. The tic marks along the noon-midnight and the dawn-dusk meridians indicate 10° intervals between 50° - 90° invariant latitudes. The sharp increase in rms phase deviation exceeding 5 radians over a narrow latitude swath (65° - 67.5° Λ) between the pre-midnight and dawn periods is the most conspicuous feature of the plots. This

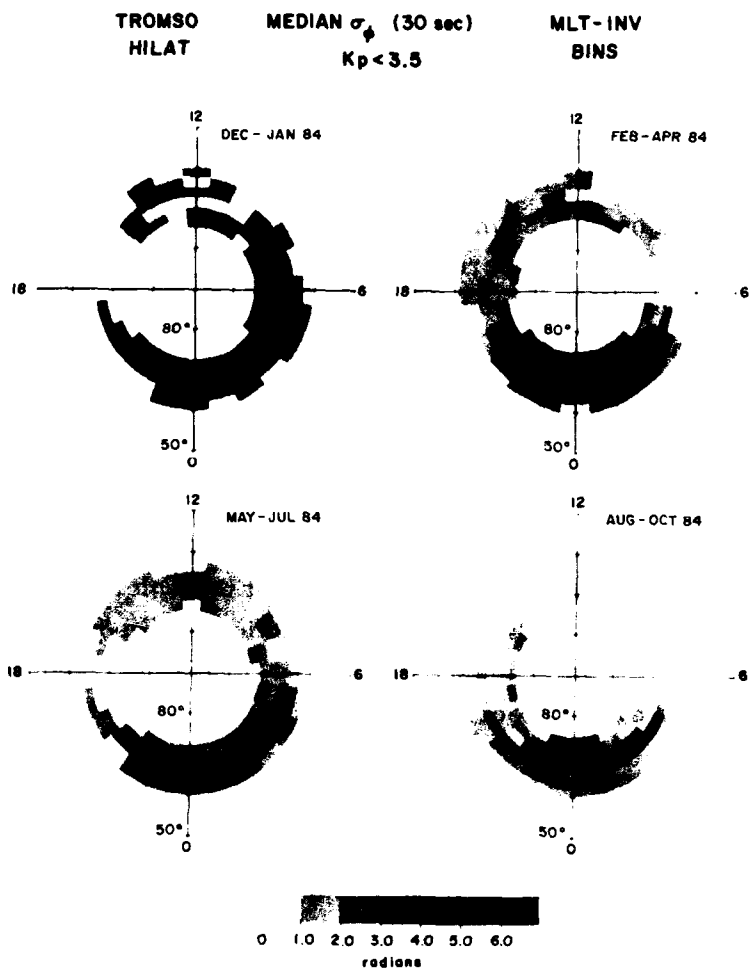

Figure 3. Seasonal Variation of Median rms Phase Deviation, σ_ϕ (137 MHz), With Invariant Latitude and Magnetic Local Time Under Quiet Magnetic Conditions During 1984

region of enhancement corresponds to the region where the alignment of the ray path with the magnetic L-shell occurs (Fremouw et al).[14] This location also coincides with the position of the diffuse aurora (Hardy et al),[15] a point we will discuss later. It is interesting to note that in a companion report, Weimer[16] has shown that

14. Fremouw, E.J., Rino, C.L., Livingston, R.C., and Cousins, M.D. (1977) A persistent subauroral scintillation enhancement observed in Alaska, Geophys. Res. Lett., 4:539.

15. Hardy, D.A., Gussenhoven, M.S., and Holeman, E. (1985) A statistical model of auroral electron precipitation, J. Geophys. Res., 90:4229.

16. Weimer, D.R. (1987) Large-scale Plasma Density Fluctuations Measured With the HiLat Satellite at 830 km Altitude, AFGL-TR-87-0110 ADA 183043, Air Force Geophysics Laboratory, Hanscom AFB, MA.

medium scale blobs (~60 km) with $\Delta N/N$ of 10 percent maximize at exactly the same 2.5° latitude bin on the nightside. It is possible that km-scale irregularities are associated with the edges of these blobs. Thus a combination of high irregularity amplitude and favorable geometry contributes to the pronounced increase of phase scintillations. The magnitude of phase scintillations during winter is found to be larger than summer. This appears somewhat intriguing because the TEC (to be shown later) was higher in summer. This leads us to conclude that the irregularities are probably less preponderant during summer in the presence of enhanced ionization of the underlying E-region. Larger phase deviations, σ_ϕ, and hence increased plasma density deviation observed during the vernal equinox of 1984 can be related to increased solar activity during this period as will be shown in a subsequent diagram.

Figure 4 presents the rms phase deviation, σ_ϕ, obtained during 1984 and 1985 in a different format. This figure indicates the variation of median rms phase deviation, σ_ϕ, with invariant latitude in the midnight and noon time periods only. Basically, this is obtained from a midnight-noon cut through the dial plots of Figure 3. When the number of data points in a particular bin over the noon-midnight sector falls below ten, the values are extrapolated from an adjacent time sector. Figure 4 illustrates an overall decrease of scintillations in 1985 due to decreased solar activity.

3.2 Phase Spectral Strength, T_ϕ

Figure 5 shows the behavior of the spectral strength, T_ϕ, of phase scintillations during 1984. The phase spectral strength is obtained from the phase spectra and corresponds to the power spectral density at 1 Hz. A midnight-noon cut of the spectral strength dial plot (Figure 5) is shown in Figure 6, with the addition of 1985 data. The levels of T_ϕ in the diagram may be properly interpreted by considering that the noise level of the phase spectra corresponds to about -50 dB. Figure 4 indicates that T_ϕ becomes maximum in the nighttime sector over the latitude swath of 65° - 67.5° Λ where the rms phase deviation, σ_ϕ, also becomes maximum as discussed in the previous section. However, the enhanced T_ϕ is considerably more extended in latitude than σ_ϕ. It seems that T_ϕ being evaluated at 1 Hz corresponds to an irregularity scale size of about 3 km whose sheet-like anisotropy is less pronounced than the larger irregularities with tens of km scale sizes that control the magnitude of σ_ϕ.

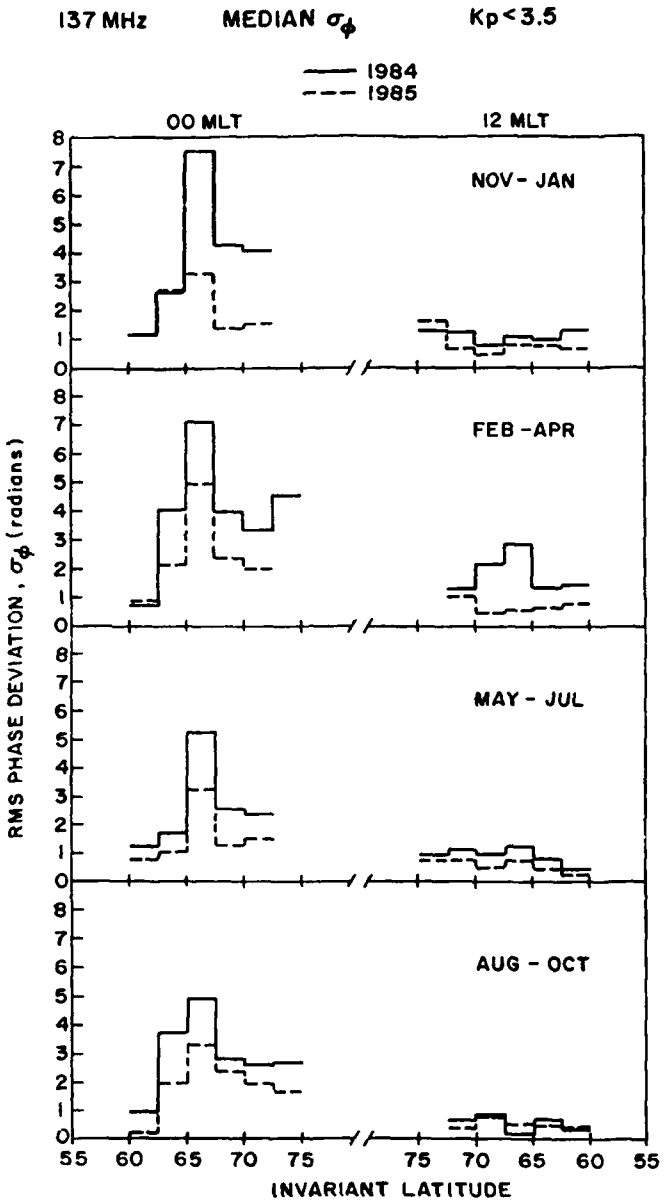

Figure 4. Seasonal Variation of Median rms Phase Deviation, σ_ϕ, (137 MHz), With Invariant Latitude Along the Midnight-Noon Meridian Under Quiet Magnetic Conditions in 1984 and 1985

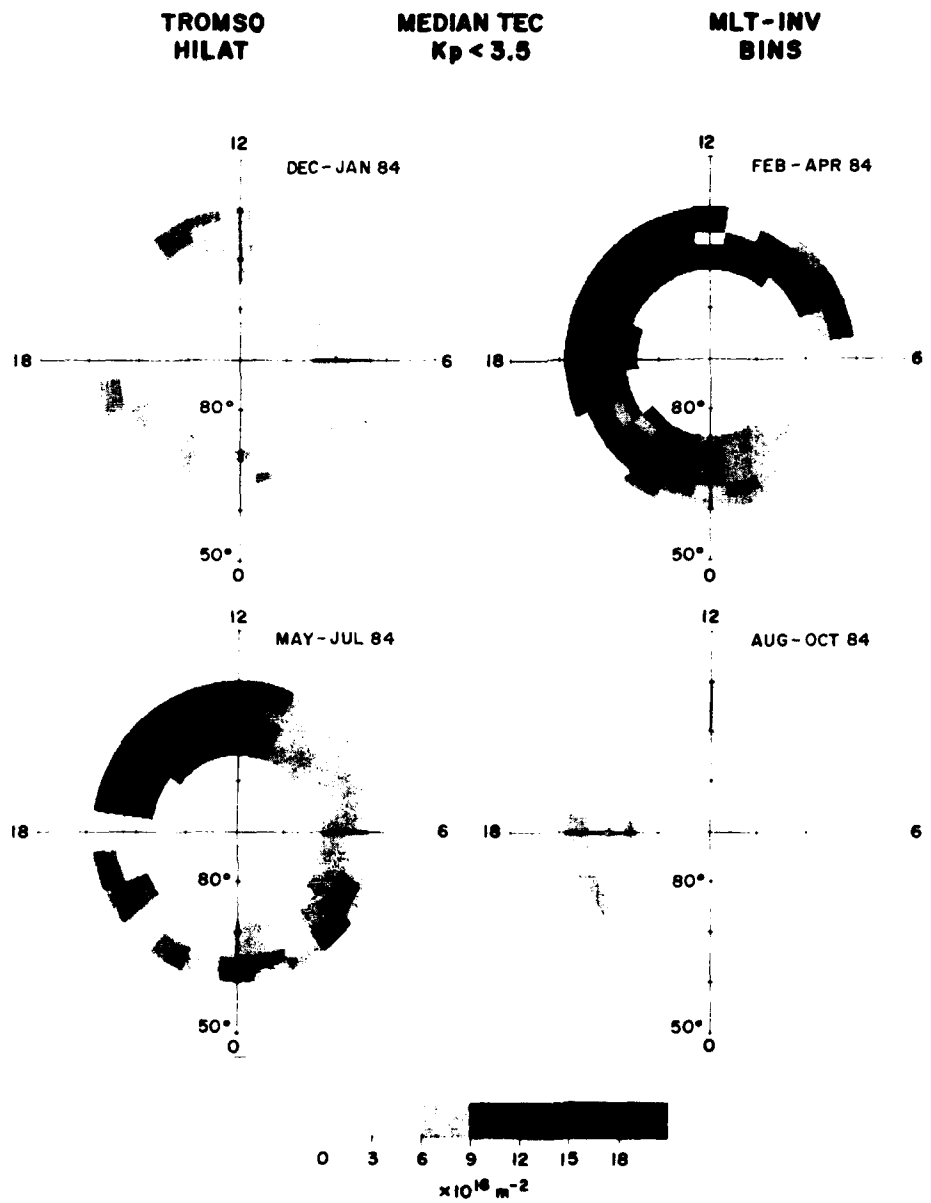

Figure 5. Seasonal Variation of Median 137 MHz Phase Spectral Strength, T_ϕ, With Invariant Latitude and Magnetic Local Time Under Quiet Magnetic Conditions During 1984

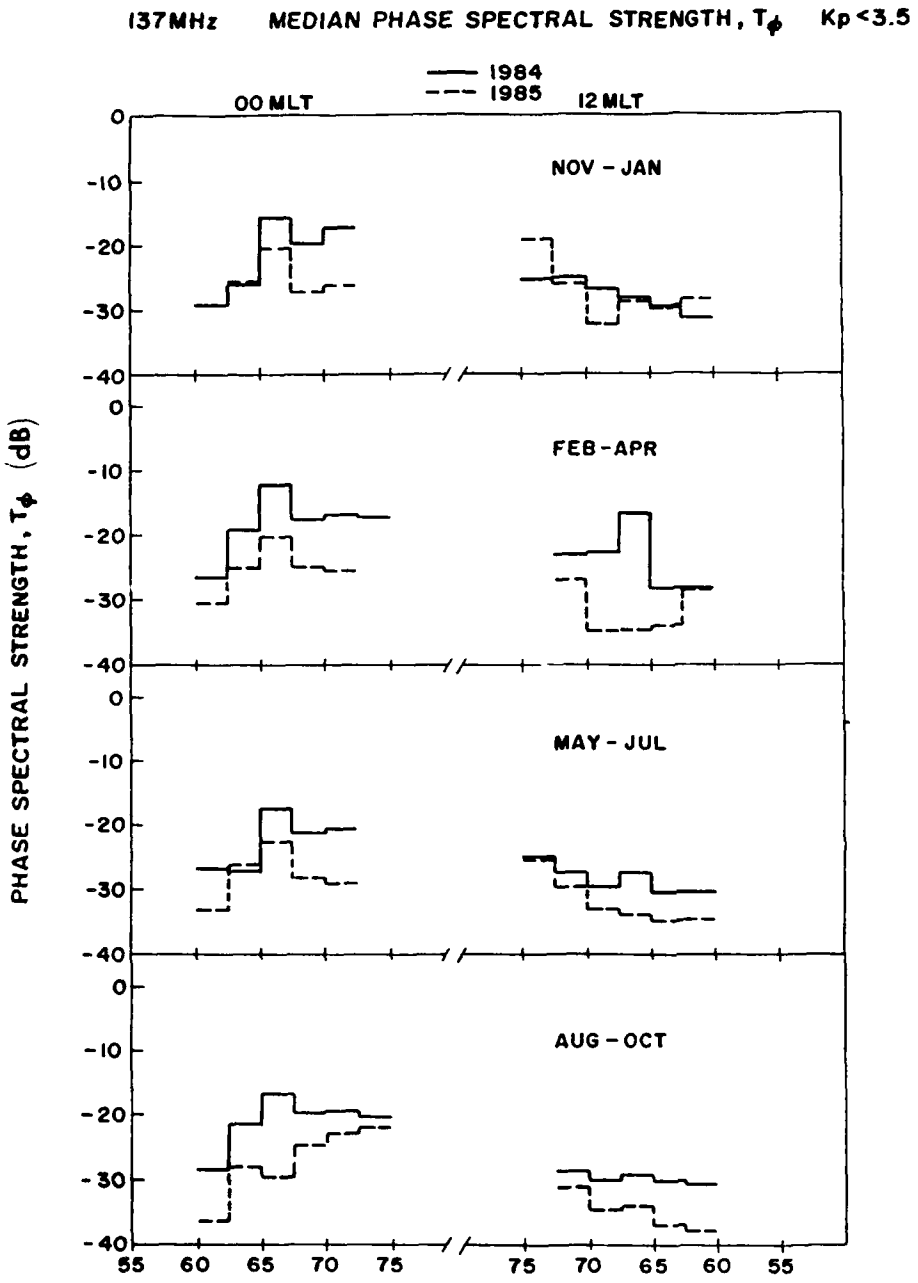

Figure 6. Seasonal Variation of Median 137 MHz Phase Spectral Strength, T_ϕ, With Invariant Latitude Along the Midnight-Noon Meridian Under Quiet Magnetic Conditions in 1984 and 1985

3.3 Phase Spectral Slope, p_ϕ

Figure 7 shows the behavior of the power law spectral index, p_ϕ, for phase scintillations at 137 MHz during 1984. A linear least square fit to the phase spectrum indicating the variation of the logarithm of power spectral density (psd) with the logarithm of frequency is obtained over the frequency interval of 0.2 Hz to 10 Hz as mentioned earlier. The best-fit line provides p_ϕ as it defines the dependence of psd on frequency f as psd $\propto f^{-p_\phi}$. Considering the scan velocity of the ray path through the F-region, the fit range 0.2 Hz to 10 Hz corresponds to the scale size regime of about 15 km to 300 m for isotropic irregularities. This regime encompasses the dominant structures that cause phase and intensity scintillations at VHF and UHF over the observing data interval. Figure 8 presents the midnight-noon cut of the dial plot of power-law spectral index, p_ϕ, with the addition of the 1985 data.

From Figures 7 and 8, it may be noted that the phase spectral index is least affected by the propagation geometry and does not show significant variations with season and solar activity in contrast to the behavior of σ_ϕ. There exists, however, a tendency for p_ϕ to increase around 65° Λ, during the nighttime. Since this location corresponds to the average location of the diffuse auroral oval as mentioned earlier, the associated E-region conductivity may account for the damping of the short scale irregularities and causing the phase spectrum to steepen (Vickrey and Kelley).[17] This steepening may also arise from increased psd at larger scales in the geometrical enhancement region due to better L-shell alignment of large scale irregularities as noted in connection with the increased σ_ϕ. The enhancements of p_ϕ are, however, smooth and distributed in contrast to the sharp geometrical enhancements of σ_ϕ. Probably, the spectral steepening arises from an interplay of both geophysical and geometrical effects.

---

17. Vickrey, J.F., and Kelley, M.C. (1982) The effects of a conducting E-layer on classical F-region cross-field plasma diffusion, J. Geophys. Res., 87:4461.

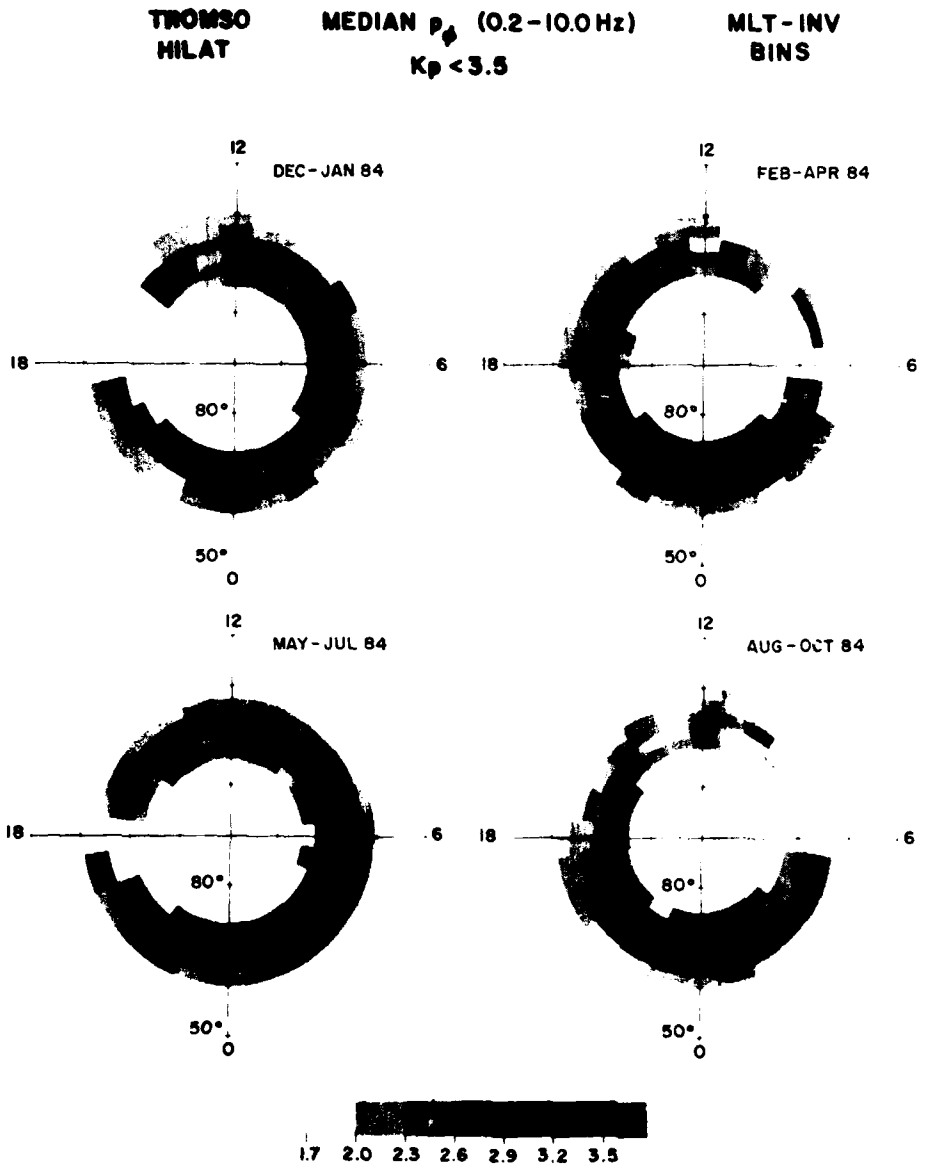

Figure 7. Seasonal Variation of Median 137 MHz Phase Spectral Slope, p_ϕ (0.2 - 10 Hz), With Invariant Latitude and Magnetic Local Time Under Quiet Magnetic Conditions During 1984

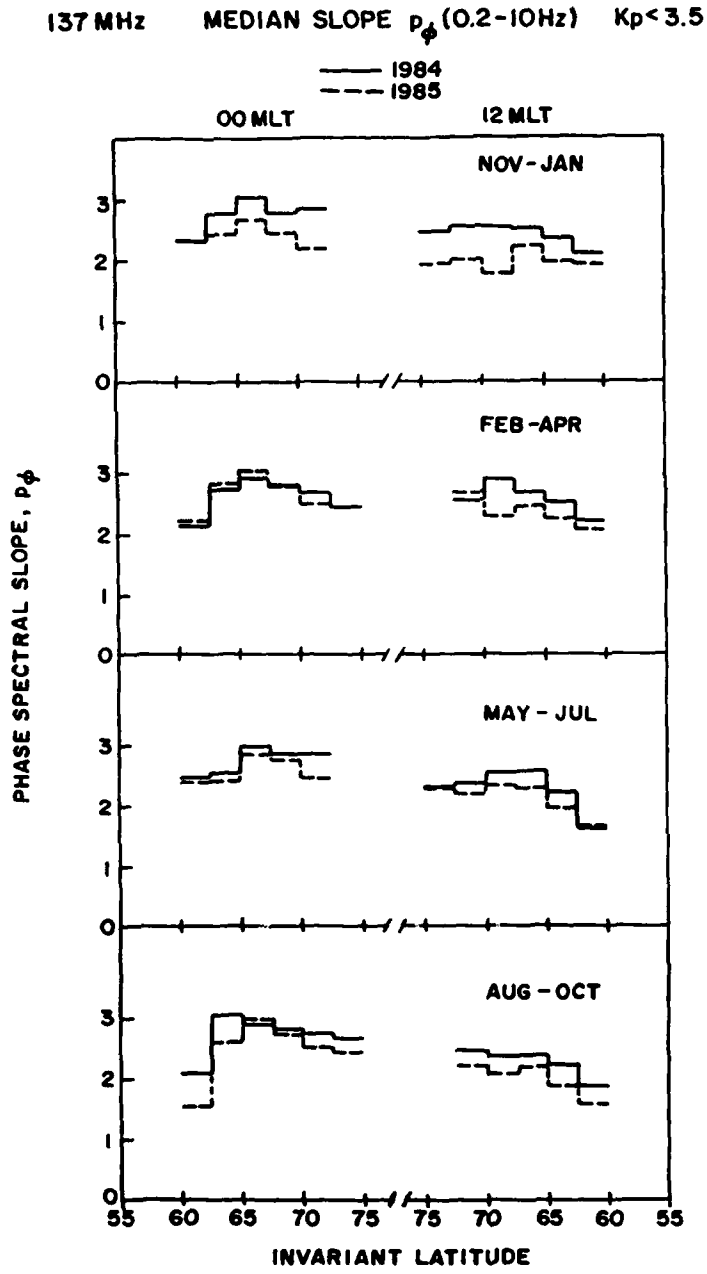

Figure 8. Seasonal Variation of Median 137 MHz Phase Spectral Slope, p_ϕ (0.2 - 10 Hz), With Invariant Latitude Along the Midnight-Noon Meridian Under Quiet Magnetic Conditions in 1984 and 1985

3.4 Intensity Scintillation Index, S_4

The intensity scintillation magnitudes have been expressed in terms of the standard S_4 index, defined as the normalized variance of signal intensity (Briggs and Parkin).[11] As mentioned earlier, a $(\sec i)^{1/2}$ variation of S_4 with ionospheric zenith angle has been removed prior to statistical processing. Figure 9 shows the variation of median S_4 at 137 MHz with invariant latitude and MLT. The nighttime enhancement of intensity scintillation index, S_4, in the region of alignment of the ray path with the magnetic L-shell (65° - 67.5°Λ) is observed to be much less pronounced when it is compared to the rms phase deviation σ_ϕ, enhancements shown in Figure 3. This indicates that the L-shell alignment of km-scale irregularities causing intensity scintillations is considerably less than the irregularities in the tens of kilometers scale that control the σ_ϕ values.

Figure 10 shows the midnight-noon cut of the dial plots of Figure 9 with the addition of 1985 data. The decrease in intensity scintillation with decrease in solar activity is in keeping with that of the rms phase deviation shown in Figure 4.

Putting these intensity scintillation index, S_4, results in perspective with other data sets, Basu and Aarons[3] had hypothesized that the seasonal variation of S_4 in the Scandinavian sector would not be as dramatic as seen at Narssarssuaq, Greenland (64° Λ). The Narssarssuaq data base, compiled from 137 MHz observations of ATS-3 during 1968-1974 (a high solar flux period), showed a strong seasonal pattern. The ATS-3 observations indicated that during the Feb - Apr period a nighttime maximum value of mean $S_4 = 0.5$ was obtained which decreased to $S_4 \approx 0.25$ in winter. More recently, Kersley et al[18] have shown observations from Kiruna at 150 MHz of intensity scintillation, S_4, during Sept 1984 - Dec 1985. In this data base, the nighttime maximum over the range 60 - 72.5° CGMLAT occurs at ~65° with median $S_4 \sim 0.2$. The winter data shows a slightly lower median S_4.

---

18. Kersley, L., Pryse, S.E., and Wheadon, N.S. (1986) Radio-wave Scintillations and Ionospheric Irregularities at High Latitudes, Rpt. Department of Physics, University College of Wales, Aberystwyth, U.K.

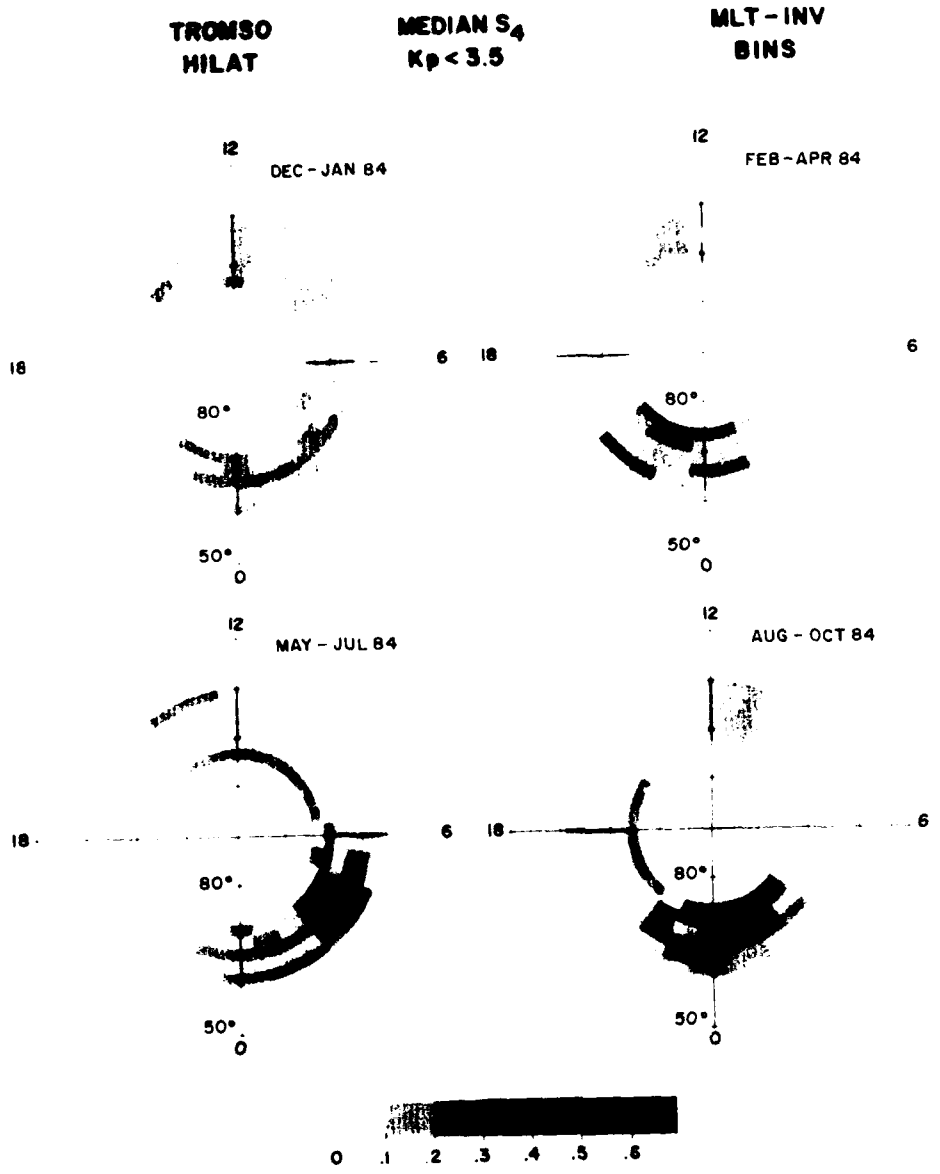

Figure 9. Seasonal Variation of Median Intensity Scintillation Index, S_4, at 137 MHz With Invariant Latitude and Magnetic Local Time Under Quiet Magnetic Conditions During 1984

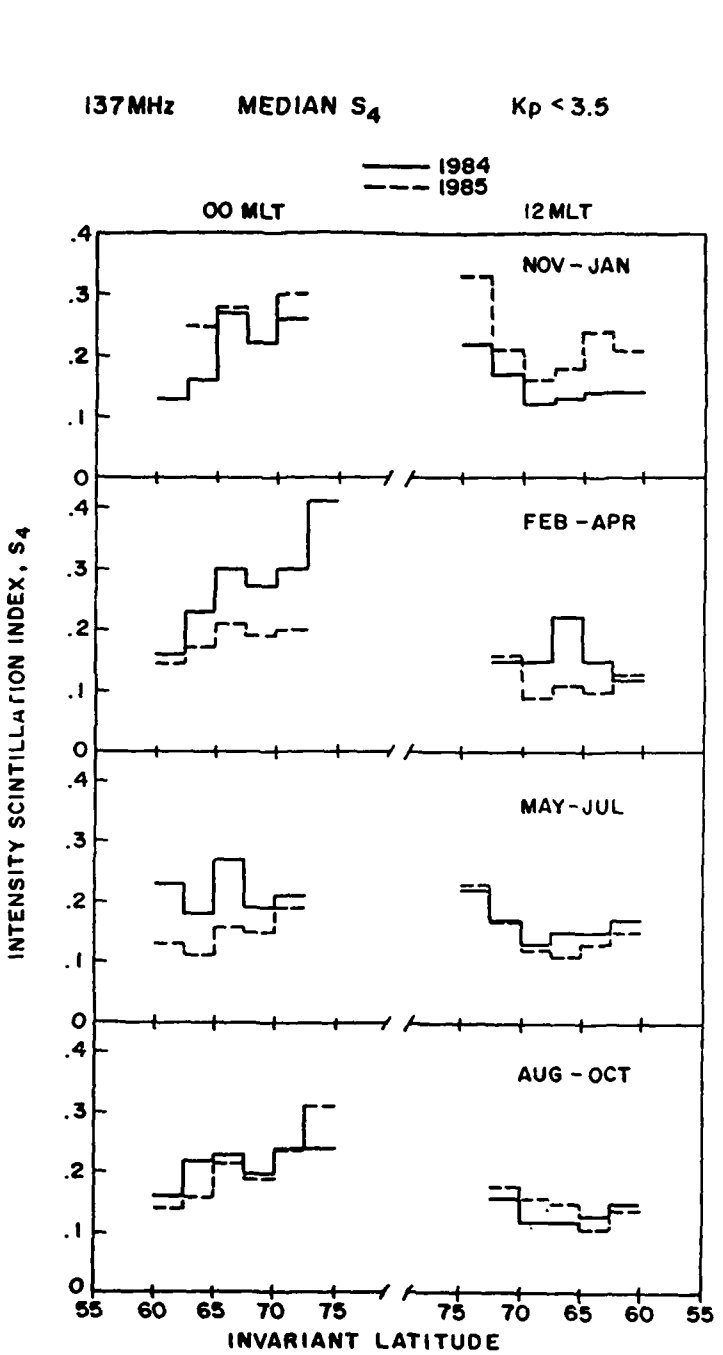

Figure 10. Seasonal Variation of Median Intensity Scintillation Index, S_4, at 137 MHz With Invariant Latitude Along the Midnight-Noon Meridian Under Quiet Magnetic Conditions in 1984 and 1985

3.5 Decorrelation Time, τ

Decorrelation time, τ, is computed as the time delay in seconds for the intensity signal to reach a decorrelation level of 0.5. For orbiting satellites, such as HiLat, the decorrelation time is dictated by the effective velocity of the satellite at F-region heights as well as the electron density structure. The effective velocity is determined by the irregularity anisotropy and the scan velocity of the ray path through the ionosphere (Rino).[19] The midnight cut of decorrelation time for the available range of invariant latitudes is shown in Figure 11. When the intensity scintillation index S_4 is low, decorrelation times cannot be measured accurately. Hence, daytime decorrelation times are not shown. The decrease of decorrelation time to values as low as 0.25 is obtained at 65 - 67.5° Λ where the intensity scintillation index, S_4, becomes maximum. This position corresponds to the alignment of the ray path the magnetic L-shell. The effective velocity becomes maximum at the above position which probably causes a decrease of the decorrelation time.

3.6 TEC (Total Electron Content)

The comb of three UHF transmissions from HiLat is used to derive the total electron content of the ionosphere up to the satellite altitude of 830 km by the differential Doppler technique (Fremouw et al).[20] In Figure 12 is shown the variation of median TEC with invariant latitude and MLT while Figure 13 shows the latitude variation of median TEC values during the noon and midnight cut of the dial plot shown in Figure 12 for different seasons in 1984 and 1985. The next diagram, Figure 14, shows the observed variation of noontime TEC in relation to the sunspot number. The effects of solar activity and season on TEC appear to be coupled. At high latitudes, owing to the near vertical orientation of the earth's magnetic field, the ionospheric irregularities of electron density at F-region heights usually extend in altitude. The integrated effect of the irregularities on radio wave propagation, such as scintillation, is therefore weighted by the total electron content of the ionosphere. Thus measurements of irregularity amplitude, $\Delta N/N$ (ΔN being the rms electron density fluctuation and N the background density), and total electron content may form the basis for a modeling of scintillation magnitudes.

Median foF2 data from Sodankyla (63° CGM) (S. Kirkwood, private communication, 1986) shows a similar nighttime pattern with Dec 1983 - Jan 1984 and

19. Rino, C.L. (1979) A power law phase screen model for ionospheric scintillation. 1. Weak scatter, Radio Sci., 14:1135.

20. Fremouw, E.J., Leadabrand, R.L., Livingston, R.C., Cousins, M.D., Rino, C.L., Fair, B.C., and Long, R.A. (1978) Early results from the DNA Wideband satellite experiment - complex-signal scintillation, Radio Sci., 13:167.

Nov 1984 - Jan 1985 showing minimum values (~ 2 - 3 MHz) while May - Jul 1984 is the period of maximum values (~ 5 MHz). Daytime foF2 shows much less of a seasonal pattern overall with maximum in Feb - Apr 1984 at 8 MHz.

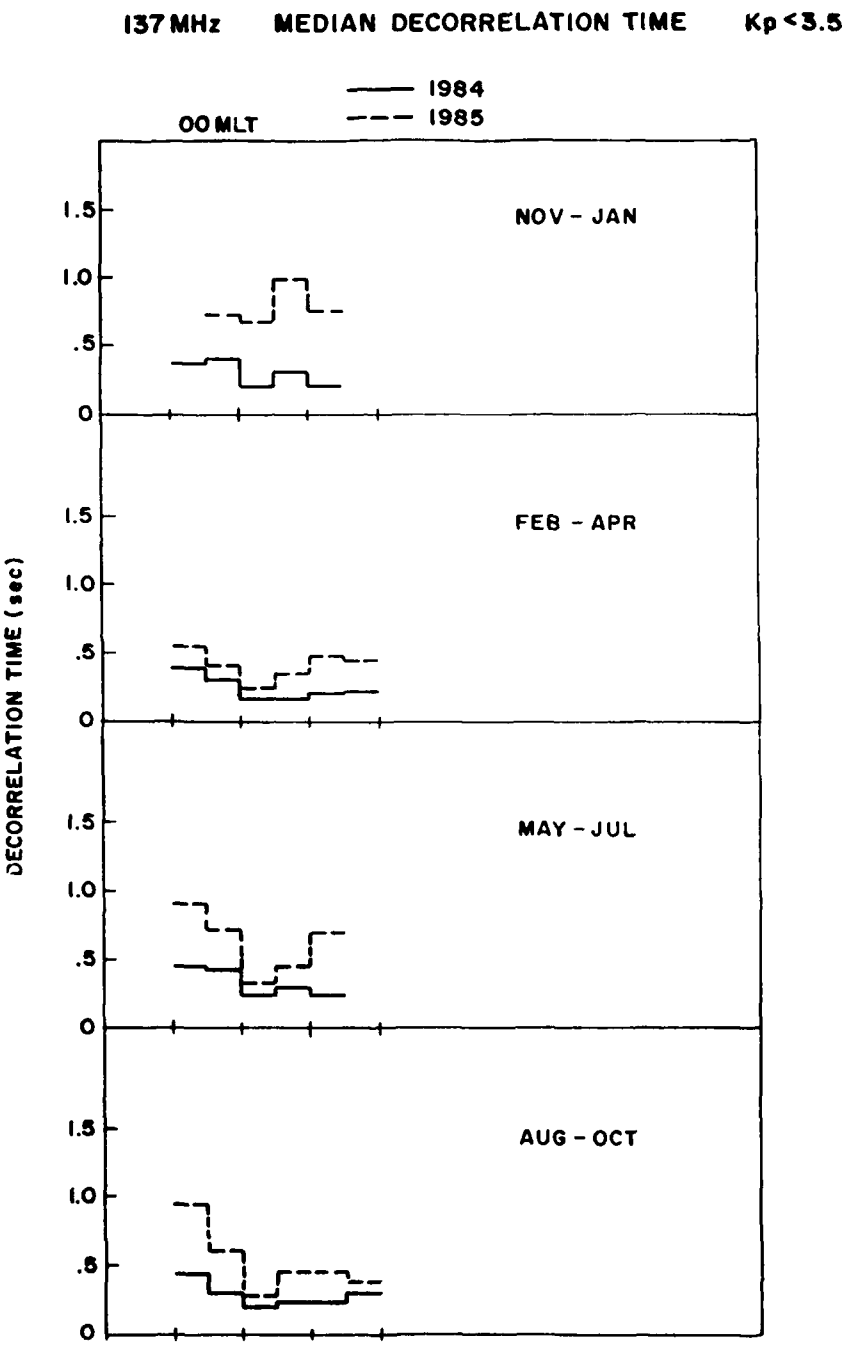

Figure 11. Seasonal Variation of Median Decorrelation Time, τ, (137 MHz) With Invariant Latitude Along the Midnight-Noon Meridian Under Quiet Magnetic Conditions in 1984 and 1985

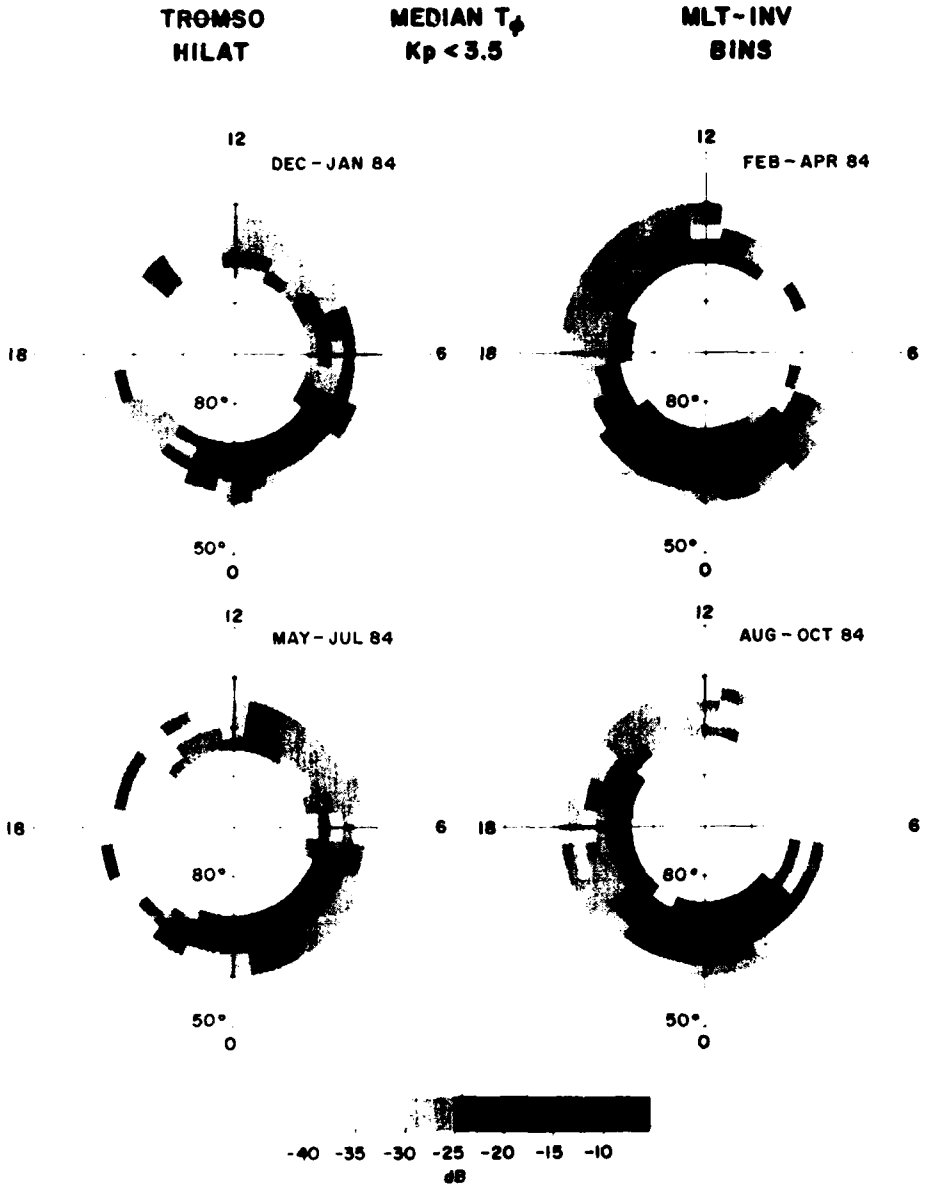

Figure 12. Seasonal Variation of Median Total Electron Content (TEC) With Invariant Latitude and Magnetic Local Time Under Quiet Magnetic Conditions During 1984

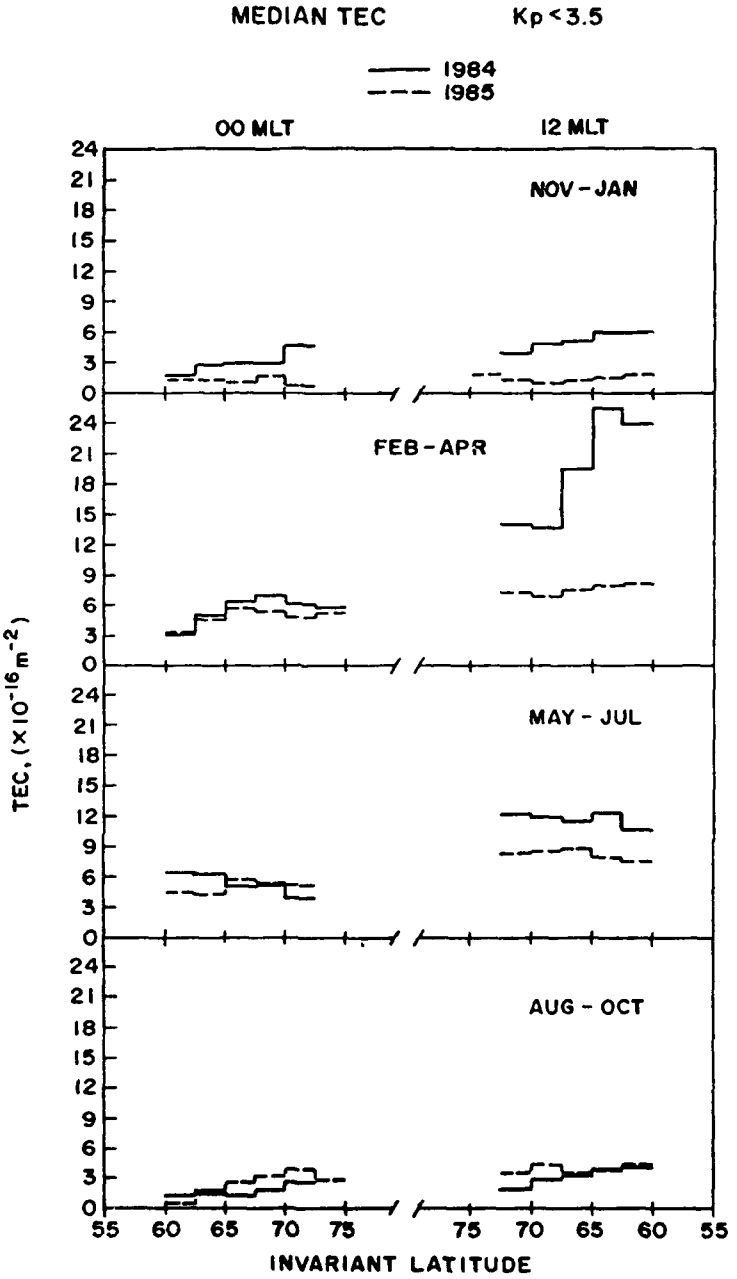

Figure 13. Seasonal Variation of Median Total Electron Content (TEC) With Invariant Latitude Along the Midnight-Noon Meridian Under Quiet Magnetic Conditions in 1984 and 1985

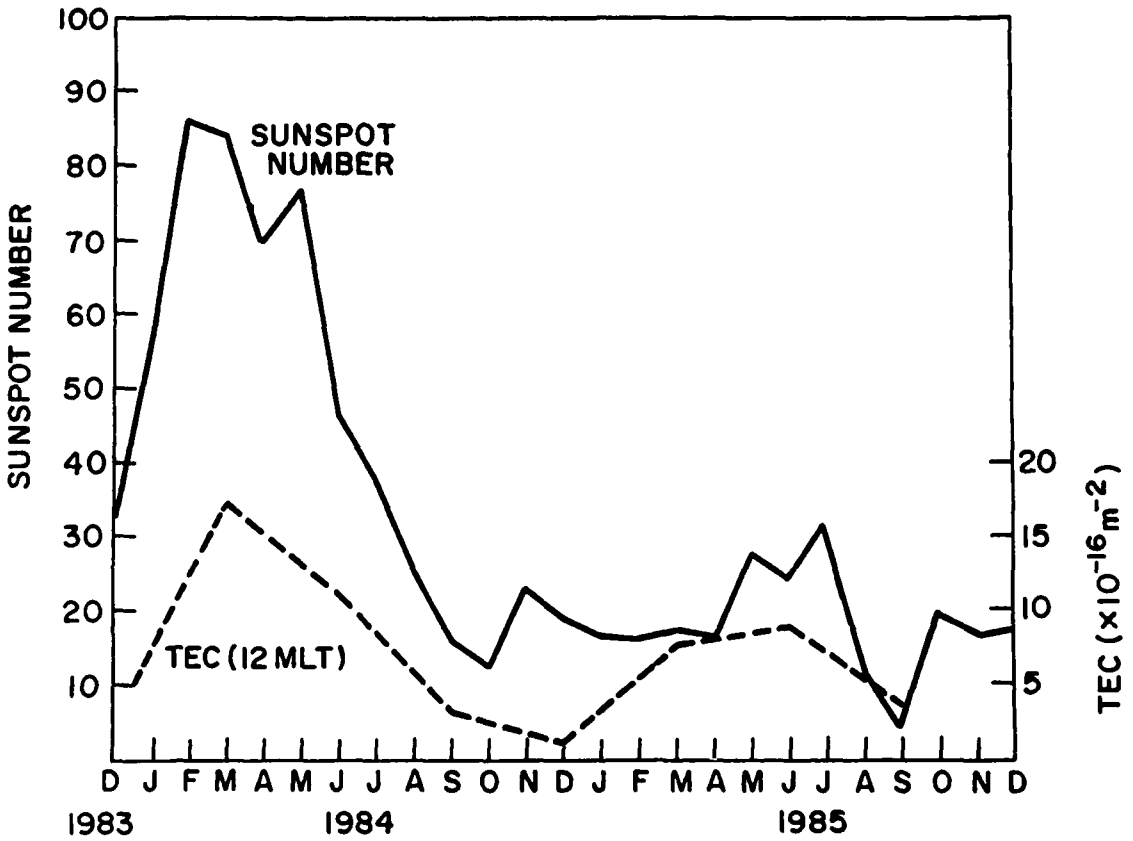

Figure 14. Illustrates the Correspondence Between the Variations of Total Electron Content and Sunspot Number

3.7 Ion Density

Among the various in-situ parameters probed by the satellite-born sensors, the in-situ ion-density measurement is an important parameter. In the F-region, due to charge neutrality, the electron and ion densities are equal. Figure 15 illustrates the invariant latitude - MLT variation of ion density during 1984 while Figure 16 shows the variation of this parameter with latitude in the midnight-noon time frame as a function of season in both 1984 and 1985 under quiet magnetic conditions. The latitudinal coverage in both Figures 15 and 16 is wider than seen in the previous figures since the ion density measurement is an in-situ parameter. The daytime ion density at 830 km is observed to follow closely the pattern of TEC variations shown earlier in Figures 12 and 13. This is seen in Table 2.

Table 2. TEC and Ion Density Measurements
67.5° Λ 12 MLT

	TEC ($\times 10^{-16}$ m^{-2})	Ion Density ($\times 10^{-10}$ m^{-3})
Nov - Jan 1984	5	0.6
Feb - Apr 1984	19	3.3
May - Jul 1984	12	2.3
Aug - Oct 1984	3	1.0
Nov - Jan 1985	1	0.3
Feb - Apr 1985	8	1.0
May - Jul 1985	9	1.3
Aug - Oct 1985	3	0.6

The ion density variations at 830 km are observed to vary with both solar activity and season.

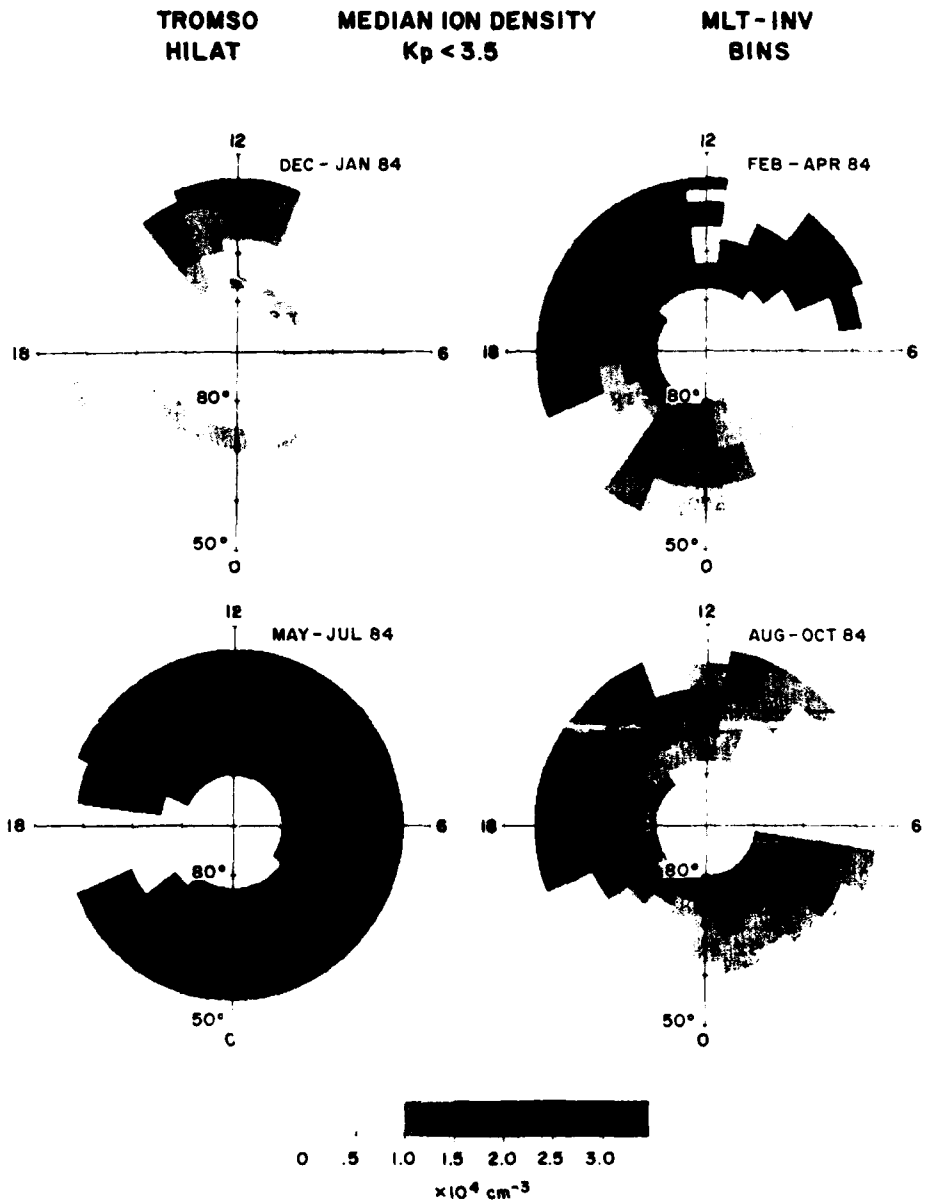

Figure 15. Seasonal Variation of Median Ion Density With Invariant Latitude and Magnetic Local Time Under Quiet Magnetic Conditions During 1984

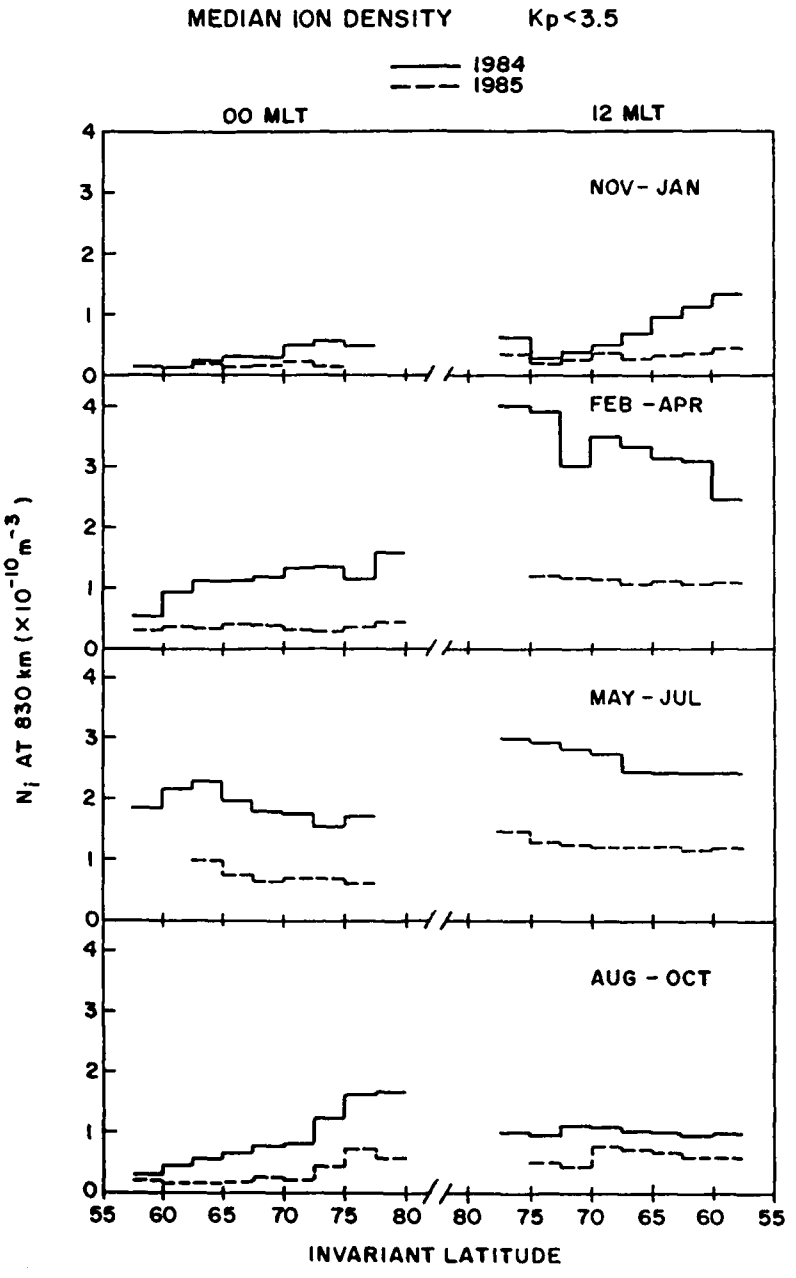

Figure 16. Seasonal Variation of Median Ion Density With Invariant Latitude Along the Midnight-Noon Meridian Under Quiet Magnetic Conditions in 1984 and 1985

Table 3 (reproduced from Rich and Smiddy)[21] illustrates a comparison of ion density observed under solar maximum conditions using the DMSP satellite in 1979 with the corresponding ion density observed under solar minimum conditions in 1984 with the HiLat satellite.

Table 3. Comparison of Median Density at 60° Magnetic Latitude Observed at 830 km Altitude by DMSP in 1979 and HiLat in 1984 (Reproduced from Rich and Smiddy)[21]

	In-situ Density $\times 10^{-4}$ cm^{-3}			
	Summer		Winter	
	1979 DMSP	1984 HiLat	1979 DMSP	1984 HiLat
Morning 07 - 11 hrs MLT	10	1.8	2.5	0.18
Evening 19 - 23 hrs MLT	10	2.5	4 to 7	0.36

3.8 Effect of Magnetic Activity

Magnetic activity, in addition to sunspot number, exerts overwhelming control of scintillations in the auroral region (Basu and Aarons[3] and Basu et al[9]). The "worst case" conditions can be illustrated by the Feb - Apr 1984 season when sunspot numbers higher than those seen in the remainder of 1984 and 1985 are coupled with magnetically disturbed conditions.

Our HiLat observations indicate that, under magnetically active conditions, scintillation magnitudes are enhanced during the nighttime and the region of enhanced activity extends in both the poleward and the equatorward directions. Irespective of the level of solar activity, scintillations are enhanced during magtic disturbances. In Figure 17 is shown the enhancement of the following parameters under magnetically disturbed conditions during Feb - Apr 1984: rms phase deviation, σ_ϕ; phase spectral strength, T_ϕ; phase spectral slope, p_ϕ; intensity scintillation index, S_4; and decorrelation time.

---

21. Rich, F.J., and Smiddy, M. (1986) Plasma Densities and Irregularities at 830-km Altitude Based on Observations During 1979, AFGL Technical Rpt. AFGL-TR-86-0121, ADA 172118, Air Force Geophysics Laboratory, Hanscom AFB, MA.

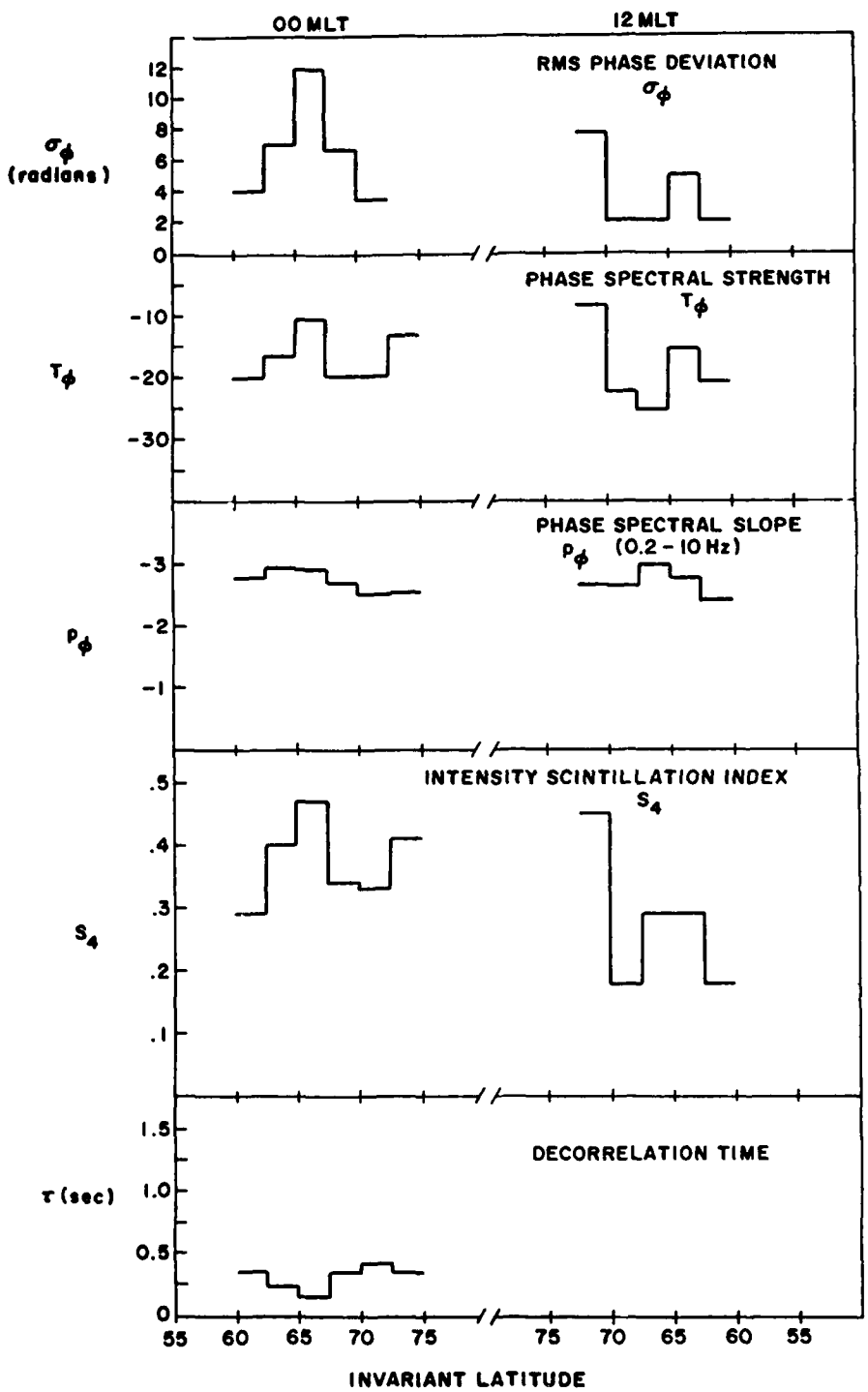

Figure 17. Variations of Scintillation Parameters: rms Phase Deviation, σ_ϕ; Phase Spectral Strength, T_ϕ; Phase Spectral Slope, p_ϕ; Intensity Scintillation Index, S_4; and Decorrelation Time, τ, Under "Worst Case" Conditions. These observations, made during Feb - Apr 1984 under disturbed magnetic conditions, are shown as a function of invariant latitude along the midnight-noon meridian

Under the "worst case" conditions, both the rms phase deviations, σ_ϕ, and the intensity scintillation index, S_4, increase by 50 percent over the scintillation level observed under quiet magnetic conditions for Feb - Apr 1984. The phase spectral slope, p_ϕ, becomes steeper and the phase spectral strength, T_ϕ, greater under disturbed magnetic conditions. No change is seen in decorrelation time, τ, possibly due to the fact that the effective scan velocity controls τ for all values of $S_4 < 0.5$.

The large increase in σ_ϕ, T_ϕ and S_4 in the 70° - 72.5° Λ latitude region in the daytime during magnetic disturbances is in all probability caused by the equatorward motion of the dayside cusp compared to its location shown in Figure 1.

4. DISCUSSION

We have shown that the most notable feature in the observed scintillation morphology at this auroral station even under magnetically quiet to moderate conditions is the enhancement of scintillations over a narrow latitude interval centered at 65° Λ in the nighttime sector. This narrow band increase of scintillations coincides with the expected region of geometrical enhancement due to the alignment of the ray path with the magnetic L-shell oriented irregularities. It is interesting to note that the boundary blobs that signify plasma density enhancements, tens of kilometers wide in the magnetic E-W direction, also occur in this region (Rino et al).[22] The spatial configuration of the blobs is controlled by the high latitude convection pattern that is mostly E-W in the auroral region (Heelis et al).[23] Robinson et al[24] have shown, with the help of simulation studies, that even a primarily circular patch of ionization being convected in from the polar cap would assume a narrow in latitude and elongated in longitude shape. These blobs can also develop small scale irregularities in their trailing edges through $\vec{E} \times \vec{B}$ instability mechanisms. In general, the plasma blobs transported from distant regions get continually structured in the convection field and control a major source of nighttime auroral scintillations.

---

22. Rino, C.L., Livingston, R.C., Tsunoda, R.T., Robinson, R.M., Vickrey, J.F., Senior, C., Cousins, M.D., Owen, J., and Klobuchar, J.A. (1983) Recent studies of the structure and morphology of auroral zone F-region irregularities, Radio Sci., 18:1167.

23. Heelis, R.A., Lowell, J.K., and Spiro, R.W. (1982) A model of the high-latitude ionospheric convection pattern, J. Geophys. Res., 87:6339.

24. Robinson, R.M., Tsunoda, R.T., Vickrey, J.F., and Guerin, L. (1985) Source of F-region ionization enhancements in the nighttime auroral zone, J. Geophys. Res., 90:7533.

The other notable finding related to the scintillation structure is the steep phase spectral slopes observed in the region of geometrical enhancement. This region coincides with the central part of the diffuse aurora under magnetically quiet conditions as has been recently shown by Hardy et al[15] from DMSP satellite observations. Unlike the limited HiLat satellite data base of particle precipitation, the DMSP satellites have provided a very large amount of data which have been organized by Hardy et al to show the characteristic variations of particle precipitation with magnetic activity. The average energy of the particle precipitation in the diffuse auroral region is on the order of a few keV that is sufficient to produce a conducting E-region. This could reduce the lifetime of small scale irregularities (~ 100 m) and contribute to the observed steepening of the phase spectral indices. Basu et al[25] have illustrated such steepening of in-situ density spectra in regions of energetic auroral particle precipitation.

The structures present in the in-situ ion density probed by the HiLat satellite have recently been investigated (Weimer).[16] This study indicates that plasma density blobs at 830 km are concentrated over a fairly narrow latitude interval. This region when mapped down the magnetic field line corresponds approximately with the region of enhanced scintillations. These results indicate that, on a statistical basis, the blobs in addition to their E-W extent are also extended along the magnetic field lines to the topside ionosphere. The altitude profiles of the blobs have been published earlier using incoherent scatter radar measurements (Vickrey et al).[26]

The extension of blobs to altitudes as high as 830 km indicates that magnetospheric coupling effects need to be included in the analysis of high latitude F-layer instabilities. The inclusion of ion-inertia in the $\vec{E} \times \vec{B}$ instability theories results in a reduction of growth rates and generation of irregularities with spectral isotropy (Mitchell et al).[27] In the non-inertial domain, the irregularity spectra become anisotropic in the north-south and the east-west directions. Thus, the irregularity spectral indices are expected to be different in the north-south and east-west directions in the non-inertial case and identical for the inertial case. At Tromso, in addition to making HiLat observations that provide a north-south scan through the ionosphere, we have performed scintillation observations with near-stationary

25. Basu, Su., Basu, S., MacKenzie, E., Coley, W.R., Hanson, W.B., and Lin, C.S. (1984) F-region electron density irregularity spectra near auroral acceleration and shear regions, J. Geophys. Res., 89:5554.

26. Vickrey, J.F., Rino, C.L., and Potemra, T.A. (1980) Chatanika/TRIAD observations of unstable ionization enhancements in the auroral F-region, Geophys. Res. Lett., 7:789.

27. Mitchell, H.G., Jr., Fedder, J.A., Keskinen, M.J., and Zalesak, S.T. (1985) A simulation of high latitude F layer instabilities in the presence of magnetosphere - ionosphere coupling, Geophys. Res. Lett., 12:283.

polar beacon satellites that provide an east-west scan controlled by ionospheric motion. The spectral indices of both sets of measurements are found to be approximately equal indicating that the inertial effects are important in the generation of kilometer scale irregularities at high latitudes that cause VHF scintillations.

Another type of auroral irregularity not associated with large-scale organized density gradients (such as to be found on the edges of blobs) but associated with velocity shears with shear gradient scale lengths ~10 km has been identified from HiLat observations (Basu et al).[28] These irregularities have somewhat shallow spectra (Basu et al)[29] as they have considerable psd at the shorter scales and can cause intense VHF scintillations at the edges of auroral arcs in association with upward field-aligned currents. Weimer[16] has shown that velocity fluctuations statistically maximize poleward of the medium scale blob structures. This is in agreement with the finding that the discrete aurora is found to map to the boundary plasma sheet and the diffuse aurora (with which the blobs are co-located) maps to the central plasma sheet in the magnetophere (Winningham et al).[30] It is tempting to associate some of the scintillations seen poleward of the geometrical enhancement region and having shallower phase spectral slopes (cf. Figures 4 and 8) with velocity shears. Keskinen et al[31] have recently shown that these velocity shears can drive the Kelvin-Helmholtz instability in both collisional and collisionless environments.

---

28. Basu, Su., Basu, S., Senior, C., Weimer, D., Nielsen, E., and Fougere, P.F. (1986) Velocity shears and sub-km scale irregularities in the nighttime auroral F-region, Geophys. Res. Lett., 13:101.

29. Basu, Su., Basu, S., MacKenzie, E., Fougere, P.F., Coley, W.R., Maynard, N.C., Winningham, J.D., Sugiura, M., Hanson, W.B., and Hoegy, W.R. (1988) Simultaneous density and electric field fluctuation spectra associated with velocity shears in the auroral oval, J. Geophys. Res., 93:115.

30. Winningham, J.D., Yasuhara, F., Akasofu, S.-I., and Heikkila, W.J. (1975) The latitudinal morphology of 10-eV to 10-keV electron fluxes during magnetically quiet and disturbed times in the 2100-0300 MLT sector, J. Geophys. Res., 80:3148.

31. Keskinen, M.J., Mitchell, H.G., Fedder, J.A., Satyanarayana, P., Zalesak, S.T., and Huba, J.D. (1988) Nonlinear evolution of the Kelvin-Helmholtz instability in the high latitude ionosphere, J. Geophys. Res., 93:137.

References

1. Aarons, J. (1982) Global morphology of ionospheric scintillations, Proc. IEEE, 70:360.
2. Basu, S., and Basu, Su. (1981) Equatorial scintillations - A review, J. Atmos. Terr. Phys., 43:473.
3. Basu, Su., and Aarons, J. (1980) The morphology of high-latitude VHF scintillation near 70° W, Radio Sci., 15:59.
4. Aarons, J., Mullen, J.P., Whitney, H., Johnson, A., and Weber, E. (1981) VHF scintillation activity over polar latitudes, Geophys. Res. Lett., 8:277.
5. Livingston, R.C. (1980) Comparison of multifrequency equatorial scintillation: American and Pacific sectors, Radio Sci., 15:801.
6. Rino, C.L., and Matthews, S.J. (1980) On the morphology of auroral zone radio wave scintillation, J. Geophys. Res., 85:4139.
7. Basu, Su., Basu, S., Livingston, R.C., Whitney, H.E., and MacKenzie, E. (1981) Comparison of Ionospheric Scintillation Statistics From the North Atlantic and Alaskan Sectors of the Auroral Oval Using the Wideband Satellite, Rep. AFGL-TR-81-0266, ADA 111871, Air Force Geophysics Laboratory, Hanscom AFB, MA.
8. Basu, Su., Basu, S., Livingston, R.C., MacKenzie, E., and Whitney, H.E. (1982) Phase and Amplitude Scintillation Statistics at 244 MHz From Goose Bay Using a Geostationary Satellite, Rep. AFGL-TR-82-0222, ADA 124291, Air Force Geophysics Laboratory, Hanscom AFB, MA.
9. Basu, Su., Basu, S., MacKenzie, E., and Whitney, H.E. (1985) Morphology of phase and intensity scintillations in the auroral oval and polar cap, Radio Sci., 20:347.
10. Fremouw, E.J., and Wittwer, L.A. (1984) The HiLat satellite program: introduction and objections, Johns Hopkins APL Technical Digest, 5:98.
11. Briggs, B.H., and Parkin, I.A. (1963) On the variation of radio star and satellite scintillation with zenith angle, J. Atmos. Terr. Phys., 25:339.

References

12. Feldstein, Y.I., and Starkov, G.V. (1967) Dynamics of auroral belt and polar geomagnetic disturbances, Planet. Space Sci., 15:209.

13. Whalen, J.A. (1970) Auroral Oval Plotter and Nomograph for Determining Corrected Geomagnetic Local Time, Latitude and Longitude for High Latitudes in Northern Hemisphere, AFCRL-70-0422, AD 713170, Air Force Geophysics Laboratory, Hanscom AFB, MA.

14. Fremouw, E.J., Rino, C.L., Livingston, R.C., and Cousins, M.D. (1977) A persistent subauroral scintillation enhancement observed in Alaska, Geophys. Res. Lett., 4:539.

15. Hardy, D.A., Gussenhoven, M.S., and Holeman, E. (1985) A statistical model of auroral electron precipitation, J. Geophys. Res., 90:4229.

16. Weimer, D.R. (1987) Large-scale Plasma Density Fluctuations Measured With the HiLat Satellite at 830 km Altitude, AFGL-TR-87-0110, ADA 183043, Air Force Geophysics Laboratory, Hanscom AFB, MA.

17. Vickrey, J.F., and Kelley, M.C. (1982) The effects of a conducting E-layer on classical F-region cross-field plasma diffusion, J. Geophys. Res., 87:4461.

18. Kersley, L., Pryse, S.E., and Wheadon, N.S. (1986) Radio-wave Scintillations and Ionospheric Irregularities at High Latitudes, Rpt. Department of Physics, University College of Wales, Aberystwyth, U.K.

19. Rino, C.L. (1979) A power law phase screen model for ionospheric scintillation. 1. Weak scatter, Radio Sci., 14:1135.

20. Fremouw, E.J., Leadabrand, R.L., Livingston, R.C., Cousins, M.D., Rino, C.L., Fair, B.C., and Long, R.A. (1978) Early results from the DNA Wideband satellite experiment - complex-signal scintillation, Radio Sci., 13:167.

21. Rich, F.J., and Smiddy, M. (1986) Plasma Densities and Irregularities at 830-km Altitude Based on Observations During 1979, AFGL Technical Rpt. AFGL-TR-86-0121, ADA 172118, Air Force Geophysics Laboratory, Hanscom AFB, MA.

22. Rino, C.L., Livingston, R.C., Tsunoda, R.T., Robinson, R.M., Vickrey, J.F., Senior, C., Cousins, M.D., Owen, J., and Klobuchar, J.A. (1983) Recent studies of the structure and morphology of auroral zone F-region irregularities, Radio Sci., 18:1167.

23. Heelis, R.A., Lowell, J.K., and Spiro, R.W. (1982) A model of the high-latitude ionospheric convection pattern, J. Geophys. Res., 87:6339.

24. Robinson, R.M., Tsunoda, R.T., Vickrey, J.F., and Guerin, L. (1985) Source of F-region ionization enhancements in the nighttime auroral zone, J. Geophys. Res., 90:7533.

25. Basu, Su., Basu, S., MacKenzie, E., Coley, W.R., Hanson, W.B., and Lin, C.S. (1984) F-region electron density irregularity spectra near auroral acceleration and shear regions, J. Geophys. Res., 89:5554.

26. Vickrey, J.F., Rino, C.L., and Potemra, T.A. (1980) Chatanika/TRIAD observations of unstable ionization enhancements in the auroral F-region, Geophys. Res. Lett., 7:789.

References

27. Mitchell, H.G., Jr., Fedder, J.A., Keskinen, M.J., and Zalesak, S.T. (1985) A simulation of high latitude F layer instabilities in the presence of magnetosphere - ionosphere coupling, Geophys. Res. Lett., 12:233.

28. Basu, Su., Basu, S., Senior, C., Weimer, D., Nielsen, E., and Fougere, P.F. (1986) Velocity shears and sub-km scale irregularities in the nighttime auroral F-region, Geophys. Res. Lett., 13:101.

29. Basu, Su., Basu, S., MacKenzie, E., Fougere, P.F., Coley, W.R., Maynard, N.C., Winningham, J.D., Sugiura, M., Hanson, W.B., and Hoegy, W.R. (1988) Simultaneous density and electric field fluctuation spectra associated with velocity shears in the auroral oval, J. Geophys. Res., 93:115.

30. Winningham, J.D., Yasuhara, F., Akasofu, S.-I., and Heikkila, W.J. (1975) The latitudinal morphology of 10-eV to 10-keV electron fluxes during magnetically quiet and disturbed times in the 2100-0300 MLT sector, J. Geophys. Res., 80:3148.

31. Keskinen, M.J., Mitchell, H.G., Fedder, J.A., Satyanarayana, P., Zalesak, S.T., and Huba, J.D. (1988) Nonlinear evolution of the Kelvin-Helmholtz instability in the high latitude ionosphere, J. Geophys. Res., 93:137.

☆ U.S. GOVERNMENT PRINTING OFFICE 1988--501-540/80047 Region #1